

Competition of Dimerization and Charge Ordering in the Spin-Peierls State of Organic Conductors

Muneo SUGIURA * and Yoshikazu SUZUMURA **

Department of Physics, Nagoya University, Nagoya 464-8602

(Received)

The effect of the charge ordering on the spin-Peierls (SP) state has been examined by using a Peierls-Hubbard model at quarter-filling with dimerization, on-site and nearest-neighbor repulsive interactions. By taking account of the presence of dimerization, a bond distortion is calculated variationally with the renormalization group method based on bosonization. When the charge ordering appears at $V = V_c$ with increasing the nearest-neighbor interaction (V), the distortion exhibits a maximum due to competition between the dimerization and the charge ordering. It is shown that the second-order phase transition occurs from the SP state with the bond alternation to a mixed state with an additional component of the site alternation at $V = V_c$.

KEYWORDS: spin-Peierls state, charge ordering, dimerization, renormalization group, bosonization, charge gap

§1. Introduction

Recently unconventional spin-Peierls (SP) states have been studied extensively for a system with a quarter-filled band, which shows a SP state in the presence of a dimerization and/or a charge ordering (CO). Typical phenomena of such a state have been found in quasi-one-dimensional organic conductors, $(\text{TMTTF})_2\text{X}$ ($\text{X}=\text{PF}_6, \text{AsF}_6$),^{1,2)} which undergo the SP transition at temperature being much lower than the CO temperature. The onset temperature of the CO state in the TMTTF salts²⁾ has been identified with the temperature corresponding to the anomaly of the dielectric constant, i.e., the temperature at which the ferroelectric transition occurs.^{3,4)} In the several features of these SP states, the present paper concerns with a coexistence and/or a competition of the SP state with the CO as maintained in the following NMR experiment on $(\text{TMTTF})_2\text{AsF}_6$.⁵⁾ With increasing pressures up to 0.15 GPa, the critical temperature of the SP state, T_{SP} , increases but that of the CO, T_{CO} , decreases where the NMR line shapes indicate a coexistence of the SP state and the CO state. For pressures larger than 0.15 GPa, T_{SP} decreases gradually while the CO is absent.

Several SP states at quarter-filling have been studied theoretically for a one-dimensional extended Hubbard model coupled with a lattice by using the variational calculation of the distortion. There are various density waves. The charge density wave (CDW) is the site-centered wave with a maximum on the lattice site and the bond order wave (BOW) is the bond-centered wave with the maximum on the bond between two neighboring lattice sites. Two kinds of SP states have been obtained depending on the location of the phase of the $2k_{\text{F}}$ wave and that of the $4k_{\text{F}}$ wave where $k_{\text{F}} (= \pi/4a)$ is the Fermi

wave vector with a being a lattice distance. One of them is a state with $2k_{\text{F}}$ BOW and $4k_{\text{F}}$ BOW (state (a)) and the other one is a state with $2k_{\text{F}}$ CDW and $4k_{\text{F}}$ CDW (state (b)) where $4k_{\text{F}}$ BOW and $4k_{\text{F}}$ CDW represent the dimerization and the CO, respectively. The state (a) corresponds to the state with $2k_{\text{F}}$ CDW2, $2k_{\text{F}}$ BOW2 and $4k_{\text{F}}$ BOW of Ung *et al.*,⁶⁾ the D_2 phase of Riera and Poilblanc,⁷⁾ and BCDW of Clay *et al.*,⁸⁾ while the state (b) corresponds to the state with $2k_{\text{F}}$ CDW1, $2k_{\text{F}}$ BOW1 and $4k_{\text{F}}$ CDW of Ung *et al.*,⁶⁾ and $4k_{\text{F}}$ CDW-SP of Clay *et al.*⁸⁾ Although the state (a) has been obtained explicitly for the large on-site repulsive interaction,⁷⁾ it is complicated to find the state (b). The fact, that the CO state relevant to the state (b) appears in the case of the large repulsive interaction between electrons of the nearest-neighbor sites, has been shown by both a numerical diagonalization⁹⁾ and a mean-field theory.¹⁰⁾ The appearance of the CO state is understood in terms of the phase Hamiltonian where the CO is followed by the change of the sign of the commensurate potential of the umklapp scattering of the quarter-filled band.^{11,12)} There arises a competition between the CO state and the SP state (i.e., the state (a)).^{8,13,14)} A phase diagram was obtained as the functions of the electron-phonon couplings for intrasite and intersite displacements of the lattice,⁸⁾ where the state (b) is obtained only in the presence of the intrasite displacement. By calculating self-consistently the state (a) in the presence of the dimerization but without the state (b), the maximum of the bond distortion was obtained at the onset of the CO.¹³⁾ The state (b) for the extended Peierls-Hubbard model (i.e., only with the intersite electron-phonon coupling) has been first discovered by Seo *et al.*¹⁴⁾ who examined the region of the CO state. Calculating self-consistently both the dimerization and the Peierls distortion, in which the phase of the Peierls distortion is taken account, they obtained a first order transition between the state (a) and the state (b), corresponding to DM+SP and CO+SP respectively

* E-mail: sugiura@slab.phys.nagoya-u.ac.jp

** E-mail: e43428a@nucc.cc.nagoya-u.ac.jp

in their notations.¹⁴⁾ Thus the competition between the dimerization and the CO is expected to exhibit a rich variety of the SP states.

In the present paper, treating the dimerization as an external field, we show the detail of the origin of the maximum of T_{SP} (the state (a)) as a function of the nearest-neighbor repulsive interaction based on our preliminary work.¹³⁾ Further we investigate the maximum of T_{SP} at the onset of the CO state by considering not only the state (b) but also the states with the arbitrary phase of the Peierls distortion.¹⁴⁾ The treatment of dimerization as the external field may be reasonable for the study of the SP state of the organic conductors, TMTTF-salts, since the dimerization does exist even at room temperatures¹⁵⁾ and T_{CO} occurs at much lower temperature. In §2, formulation is given. The Hamiltonian is expressed in terms of the bosonization and the renormalization group (RG) equations are derived to calculate the distortion, u , i.e., the order parameter of the SP state. In §3, RG flows are calculated for both the state without CO and that with CO. The distortion u is calculated as a function of the nearest-neighbor repulsive interaction where a phase of the distortion is determined to obtain the optimum u . In §4, discussion is given.

§2. Formulation

We consider a quarter-filled extended Peierls-Hubbard model with dimerization, given by

$$H = - \sum_{j=0}^{N-1} \sum_{\sigma} \{ t + (-1)^j x_d + (u_j - u_{j+1}) \} \times (c_{j,\sigma}^{\dagger} c_{j+1,\sigma} + h.c.)$$

$$+ U \sum_j n_{j,\uparrow} n_{j,\downarrow} + V \sum_{j,\sigma,\sigma'} n_{j,\sigma} n_{j+1,\sigma'}$$

$$+ \frac{K}{2} \sum_j (u_j - u_{j+1})^2, \quad (1)$$

where

$$u_j = -u \cos(\pi j/2 - \zeta), \quad (2)$$

and $n_{j,\sigma} = c_{j,\sigma}^{\dagger} c_{j,\sigma}$. Quantities u and ζ correspond to an amplitude and a phase of the Peierls distortion, respectively and $c_{j,\sigma}^{\dagger}$ denotes the creation operator for an electron with spin σ at the site j . The x_d term represents the bond dimerization while U and V are coupling constants for the repulsive interactions of on-site and that of nearest-neighbor site, respectively. The last term expresses the elastic energy induced by the distortion where K is a spring constant. We use a coupling constant $g (= 4a/\pi v_F K)$ instead of K , where v_F is the Fermi velocity. The electron band splits into an upper band and a lower band due to the dimerization x_d , where the lower band is linearized to study the state close to the Fermi point. By applying the bosonization method,

we define phase variables $\theta_{\pm}(x)$ and $\phi_{\pm}(x)$ as

$$\begin{pmatrix} \theta_{\pm} \\ \phi_{\pm} \end{pmatrix} = \sum_{\substack{\sigma=\pm(\uparrow\downarrow) \\ q \neq 0}} \frac{\pi i}{qL} e^{-\alpha|q|/2 - iqx} [\rho_{+,\sigma}(q) \pm \rho_{-,\sigma}(q)] \begin{pmatrix} 1 \\ \sigma \end{pmatrix}, \quad (3)$$

where the notation $\sigma = +(-)$ denotes spin for $\uparrow(\downarrow)$ and $\rho_{+(-),\sigma}$ represents the density operator for the right going (left going) electrons. The density operators $\rho_{+(-),\sigma}(q)$ satisfy the boson commutation relation, $[\rho_{\pm,\sigma}(-q), \rho_{\pm,\sigma'}(q')] = \pm(qL/2\pi)\delta_{q,q'}\delta_{\sigma,\sigma'}$. In eq. (3), θ_+ and ϕ_+ represent the charge fluctuation and the spin fluctuation, respectively, since $\pi^{-1}\partial\theta_+/\partial x$ ($\pi^{-1}\partial\phi_+/\partial x$) expresses the charge density (spin density).¹⁶⁾ They satisfy the commutation relation, $[\theta_+(x), \theta_-(x')] = [\phi_+(x), \phi_-(x')] = i\pi \text{sgn}(x - x')$. Using phase variables, the operator for the right going (left going) electron, $p = +(-)$, is written as¹⁶⁻¹⁸⁾

$$\psi_{p,\sigma}(x) = \frac{1}{\sqrt{2\pi\alpha}} \exp \left[ipk_F x + ip [\theta_+ + p\theta_- + \sigma(\phi_+ + p\phi_-)]/2 \right] e^{i\Xi_{p,\sigma}}, \quad (4)$$

where $c_{j,\sigma} = \sqrt{a}(\psi_{+,\sigma}(x) + \psi_{-,\sigma}(x))$ with $x = aj$ and the lattice constant a . In eq.(4), $\Xi_{+,\uparrow} = \pi(N_{+,\uparrow} + N_{-,\uparrow})/2$, $\Xi_{-,\uparrow} = -\pi(N_{+,\uparrow} + N_{-,\uparrow})/2$, $\Xi_{+,\downarrow} = \pi(N_{+,\uparrow} + N_{-,\uparrow}) + \pi(N_{+,\downarrow} + N_{-,\downarrow})/2$, $\Xi_{-,\downarrow} = \pi(N_{+,\uparrow} + N_{-,\uparrow}) - \pi(N_{+,\downarrow} + N_{-,\downarrow})/2$ and $N_{p,\sigma} = \int dx \psi_{p,\sigma}^{\dagger} \psi_{p,\sigma}$. In terms of these phase variables, eq. (1) is rewritten as,^{11, 16-19)}

$$H = H_0 + H_1, \quad (5)$$

$$H_0 = \frac{v_{\rho}}{4\pi} \int dx \left[\frac{1}{K_{\rho}} (\partial_x \theta_+)^2 + K_{\rho} (\partial_x \theta_-)^2 \right]$$

$$+ \frac{v_{\sigma}}{4\pi} \int dx \left[\frac{1}{K_{\sigma}} (\partial_x \phi_+)^2 + K_{\sigma} (\partial_x \phi_-)^2 \right], \quad (6)$$

$$H_1 = \frac{v_F}{2\pi\alpha^2} \int dx \left[y_{1/4} \cos 4\theta_+ - y_{1/2} \sin 2\theta_+ + y_{\sigma} \cos 2\phi_+ - (4\sqrt{2}\alpha u/v_F) \sin(\theta_+ + \zeta) \cos \phi_+ + 4(\alpha u/v_F)^2/g \right], \quad (7)$$

where coefficients of the nonlinear terms are given by

$$K_{\rho} = \{1/(1 + \tilde{U} + 4\tilde{V})\}^{1/2},$$

$$K_{\sigma} = \{1/(1 - \tilde{U})\}^{1/2},$$

$$y_{1/4} = A^4(a/2\alpha)^2 \tilde{U}^2 (\tilde{U} - 4\tilde{V}),$$

$$y_{1/2} = 2(x_d/t) \tilde{U} / \{1 + (x_d/t)^2\},$$

$$y_{\sigma} = \tilde{U}. \quad (8)$$

The quantities v_{ρ} and v_{σ} are velocities given by $v_{\rho} = v_F(1 + \tilde{U} + 4\tilde{V})^{1/2}$ and $v_{\sigma} = v_F(1 - \tilde{U})^{1/2}$ where $v_F = \sqrt{2ta}\{1 - (x_d/t)^2\}/\{1 + (x_d/t)^2\}^{1/2}$, $\tilde{U} = Ua/(\pi v_F)$, $\tilde{V} = Va/(\pi v_F)$ and $A = \{1 - (x_d/t)^2\}/\{1 + (x_d/t)^2\}$. The quantity K_{ρ} (K_{σ}) expresses the degree of the charge (spin) fluctuation. The amplitude, $y_{1/2}$, originates in

the umklapp scattering of half-filling due to the dimerization while $y_{1/4}$ denotes that of quarter-filling obtained by integrating the contribution from upper band.¹¹⁾ The quantity y_σ denotes the backward scattering. The cutoff parameter, α , is of the order of the lattice constant and is taken as $\alpha = 1.9a/\pi$ for quarter-filling.¹¹⁾ In terms of phase variables, the order parameters of $2k_F$ CDW, $4k_F$ CDW and $4k_F$ BOW are written as

$$\begin{aligned} O_{2k_F \text{CDW}} &= \sum_{p,\sigma} \psi_{p,\sigma}^\dagger(x) \psi_{-p,\sigma}(x) \\ &= \frac{2}{\pi\alpha} \cos(2k_F x + \theta_+) \cos \phi_+, \end{aligned} \quad (9)$$

$$\begin{aligned} O_{4k_F \text{CDW}} &= - \sum_p \psi_{p,\uparrow}^\dagger(x) \psi_{p,\downarrow}^\dagger(x) \psi_{-p,\downarrow}(x) \psi_{-p,\uparrow}(x) \\ &= - \frac{1}{2\pi^2\alpha^2} \cos(4k_F x + 2\theta_+) , \end{aligned} \quad (10)$$

$$\begin{aligned} O_{4k_F \text{BOW}} &= - \sum_p \psi_{p,\uparrow}^\dagger\left(x - \frac{a}{2}\right) \psi_{p,\downarrow}^\dagger\left(x + \frac{a}{2}\right) \\ &\quad \times \psi_{-p,\downarrow}\left(x - \frac{a}{2}\right) \psi_{-p,\uparrow}\left(x + \frac{a}{2}\right) \\ &= \frac{1}{2\pi^2\alpha^2} \sin\left(4k_F\left(x - \frac{a}{2}\right) + 2\theta_+\right) . \end{aligned} \quad (11)$$

The variable x of eqs. (9) and (10), is defined at the lattice site while that of eq. (11) is defined on the bond, i.e. $x = a/2, 3a/2, \dots$. Equations (9) and (11) for $\theta_+ \rightarrow \pi/4$ show the $2k_F$ BOW and $4k_F$ BOW while eqs. (9) and (10) for $\theta_+ \rightarrow \pi/2$ represent $2k_F$ CDW and $4k_F$ CDW.

Quantities u and ζ in eq. (7) are determined so as to minimize $\langle H \rangle$ leading to two kinds of conditions, $\langle \partial H / \partial u \rangle = 0$ and $\langle \partial H / \partial \zeta \rangle = 0$. The condition, $\langle \partial H / \partial u \rangle = 0$, is written as

$$\begin{aligned} \frac{\sqrt{2}\alpha}{gv_F} u &= F \equiv \langle \sin(\theta_+ + \zeta) \cos \phi_+ \rangle \\ &= \cos \zeta \langle \sin \theta_+ \cos \phi_+ \rangle + \sin \zeta \langle \cos \theta_+ \cos \phi_+ \rangle , \end{aligned} \quad (12)$$

where F is calculated as the function of u and ζ from eq. (5). Instead of the condition of $\langle \partial H / \partial \zeta \rangle = 0$, we use a condition of optimizing u with respect to ζ , i.e., $du/d\zeta = 0$, which is discussed later. It is noted that F is expressed in terms of the original Hamiltonian as

$$\begin{aligned} F &= - \frac{\pi}{2N} \sum_{j,\sigma} \left\langle \sin\left(\frac{\pi j}{2} - \zeta + \frac{\pi}{4}\right) \right. \\ &\quad \left. \times (c_{j,\sigma}^\dagger c_{j+1,\sigma} + h.c.) \right\rangle . \end{aligned} \quad (13)$$

The quantity u is determined to satisfy the relation, $(\sqrt{2}\alpha/gv_F)u = F$. The quantity F of the r.h.s. of eq. (12) is evaluated by making use of the RG method, in which u is taken into account as the initial value. In order to derive the RG equations, eq. (5) is replaced by an effective Hamiltonian, $H^{\text{eff}} = H_0 + H_1^{\text{eff}}$, where H_1^{eff} is written as

$$H_1^{\text{eff}} = \frac{v_F}{2\pi\alpha^2} \int dx \left[y_{1/4} \cos 4\theta_+ - y_{1/2} \sin 2\theta_+ \right.$$

$$\begin{aligned} &- y_{2\rho} \cos 2\theta_+ + y_\sigma \cos 2\phi_+ \\ &- y_{ps} \sin \theta_+ \cos \phi_+ - y_{pc} \cos \theta_+ \cos \phi_+ \\ &\left. + (y_{ps}^2 + y_{pc}^2)/8g \right] , \end{aligned} \quad (14)$$

where

$$\begin{aligned} y_{ps} &= (4\sqrt{2}\alpha u/v_F) \cos \zeta , \\ y_{pc} &= (4\sqrt{2}\alpha u/v_F) \sin \zeta , \end{aligned} \quad (15)$$

and the $y_{2\rho}$ term is induced through the RG process with increasing the length of the scale, i.e., αe^l . By applying a transformation, $\alpha \rightarrow \alpha(1 + dl)$, to coefficients of eq. (14),^{19–22)} one obtains RG equations as (Appendix)

$$\begin{aligned} \frac{d}{dl} K_\rho(l) &= - \left[2 y_{1/4}^2(l) + \frac{1}{2} (y_{1/2}^2(l) + y_{2\rho}^2(l)) \right. \\ &\quad \left. + \frac{1}{16} (y_{ps}^2(l) + y_{pc}^2(l)) \right] K_\rho^2(l) , \end{aligned} \quad (16a)$$

$$\frac{d}{dl} G_\sigma(l) = - y_\sigma^2(l) - \frac{1}{8} (y_{ps}^2(l) + y_{pc}^2(l)) , \quad (16b)$$

$$\begin{aligned} \frac{d}{dl} y_{1/4}(l) &= [2 - 8 K_\rho(l)] y_{1/4}(l) \\ &\quad + \frac{1}{4} (y_{1/2}^2(l) - y_{2\rho}^2(l)) , \end{aligned} \quad (16c)$$

$$\begin{aligned} \frac{d}{dl} y_{1/2}(l) &= \left[2 - 2 K_\rho(l) + \frac{1}{2} y_{1/4}(l) \right] y_{1/2}(l) \\ &\quad + \frac{1}{4} y_{ps}(l) y_{pc}(l) , \end{aligned} \quad (16d)$$

$$\begin{aligned} \frac{d}{dl} y_{2\rho}(l) &= \left[2 - 2 K_\rho(l) - \frac{1}{2} y_{1/4}(l) \right] y_{2\rho}(l) \\ &\quad - \frac{1}{8} (y_{ps}^2(l) - y_{pc}^2(l)) , \end{aligned} \quad (16e)$$

$$\frac{d}{dl} y_\sigma(l) = - G_\sigma(l) y_\sigma(l) - \frac{1}{8} (y_{ps}^2(l) + y_{pc}^2(l)) , \quad (16f)$$

$$\begin{aligned} \frac{d}{dl} y_{ps}(l) &= \left[\frac{3}{2} - \frac{1}{2} K_\rho(l) - \frac{1}{4} G_\sigma(l) - \frac{1}{2} y_{2\rho}(l) \right. \\ &\quad \left. - \frac{1}{2} y_\sigma(l) \right] y_{ps}(l) + \frac{1}{2} y_{1/2}(l) y_{pc}(l) , \end{aligned} \quad (16g)$$

$$\begin{aligned} \frac{d}{dl} y_{pc}(l) &= \left[\frac{3}{2} - \frac{1}{2} K_\rho(l) - \frac{1}{4} G_\sigma(l) + \frac{1}{2} y_{2\rho}(l) \right. \\ &\quad \left. - \frac{1}{2} y_\sigma(l) \right] y_{pc}(l) + \frac{1}{2} y_{1/2}(l) y_{ps}(l) , \end{aligned} \quad (16h)$$

where $K_\sigma = 1 + G_\sigma/2$ and $G_\sigma = \tilde{U}$. The initial conditions ($l = 0$) for these quantities are given by eqs. (8) and (15), and $y_{2\rho}(0) = 0$. In deriving eqs. (16), v_ρ and v_σ are replaced by v_F . We note that RG equations similar to eqs. (16) have been derived by Yonemitsu,²²⁾ who treated the case of the phonon with finite frequency but without $y_{2\rho}$ and y_{pc} terms. Since eqs. (16) are the result of first order RG, the renormalized quantity increases to infin-

ity for the case of the strong coupling. Then when the renormalized quantity becomes large (e.g., $y_{1/2}, y_{2\rho}, |y_\sigma|, [y_{ps}^2 + y_{pc}^2]^{1/2} \rightarrow 2$ in the present calculation), we stop the renormalization for the corresponding quantity.

Here we estimate the quantity F of eq. (12) by employing the following response function, whose limiting value with the long distance gives F as found in the ordered state. The response function for F , which depends on both the imaginary time τ and the space x , is defined by

$$R(|\vec{r}_1 - \vec{r}_2|) = \langle T_\tau \hat{F}(\vec{r}_1) \hat{F}(\vec{r}_2) \rangle \\ = R_s \cos^2 \zeta + R_{sc} \sin 2\zeta + R_c \sin^2 \zeta, \quad (17)$$

where $\hat{F}(\vec{r}) = \cos \zeta \sin \theta_+(\vec{r}) \cos \phi_+(\vec{r}) + \sin \zeta \cos \theta_+(\vec{r}) \cos \phi_+(\vec{r})$ and $\vec{r} = (x, v_F \tau)$. Quantities R_s, R_c and R_{sc} are given by

$$R_s = \langle \sin \theta_+(r) \cos \phi_+(r) \sin \theta_+(0) \cos \phi_+(0) \rangle, \\ R_c = \langle \cos \theta_+(r) \cos \phi_+(r) \cos \theta_+(0) \cos \phi_+(0) \rangle, \\ R_{sc} = R_{cs} = \langle \sin \theta_+(r) \cos \phi_+(r) \cos \theta_+(0) \cos \phi_+(0) \rangle. \quad (18)$$

In a way similar to eqs. (16), eqs. (18) are calculated where r is replaced by $\alpha \exp(l)$. The corresponding RG equations are given by^{23, 24)} (Appendix),

$$\frac{d}{dl} R_s(l) = - \left[(K_\rho(l) + y_{2\rho}(l)) \theta(l_c - l) \right. \\ \left. + K_\sigma(l) + y_\sigma(l) \right] R_s(l) \\ + \theta(l_c - l) y_{1/2}(l) R_{sc}(l), \quad (19a)$$

$$\frac{d}{dl} R_c(l) = - \left[(K_\rho(l) - y_{2\rho}(l)) \theta(l_c - l) \right. \\ \left. + K_\sigma(l) + y_\sigma(l) \right] R_c(l) \\ + \theta(l_c - l) y_{1/2}(l) R_{sc}(l), \quad (19b)$$

$$\frac{d}{dl} R_{sc}(l) = - \left[K_\rho(l) \theta(l_c - l) + K_\sigma(l) + y_\sigma(l) \right] R_{sc}(l) \\ + \frac{1}{2} \theta(l_c - l) y_{1/2}(l) (R_s(l) + R_c(l)), \quad (19c)$$

where $R_s(0) = R_c(0) = 1/4$, $R_{sc}(0) = 0$ and $\theta(x) = 1(0)$ for $x > 0$ ($x < 0$). The quantity l_c denotes a scale at which the coupling for the charge fluctuation develops well. Then the region with $l > l_c$ is regarded as the strong coupling one where the charge fluctuation is frozen. We take $l_c = \min(l_{c1}, l_{c2})$ where the present numerical calculation for the response function gives a reasonable result with a choice of $y_{1/2}(l_{c1}) = 1$ and $|y_{1/4}(l_{c2})| = 2$ due to the first order RG. Equation (17) is estimated from eqs. (19), which are calculated by using the solution of eqs. (16). Although the quantity F corresponds to $R^{1/2}(|\vec{r}_1 - \vec{r}_2| = \infty)$, we estimate F from

the value of $R(l_m)$, i.e.,

$$F = R^{1/2}(l_m), \quad (20)$$

where l_m denotes the following characteristic length. When y_σ becomes of the order of unity due to the relevant y_{ps} and/or y_{pc} , the spin gap is formed and eq. (17) as the function of l takes a minimum at $l = l_m$ due to the first order RG. Since $R(l)$ becomes invalid for $l \geq l_m$, we replace $R(\infty)$ with $R(l_m)$. Thus, u is obtained by the following procedure. First, eq. (20) is used for estimating F with various choices of u which gives the initial value of RG equations. Next, u is calculated by relating F with u through eq. (12) which is equivalent to the Hellman-Feynman theorem. Finally, ζ is determined to give the maximum of u .

Equation (14) shows that the Peierls distortion is determined by $y_{ps}(l)$ and $y_{pc}(l)$ with the optimum ζ . Thus it is convenient to use a linear combination of y_{ps} and y_{pc} terms. In the following section, we discuss the SP state by rewriting y_{ps} and y_{pc} terms in eq. (14) as

$$\frac{v_F}{2\pi\alpha^2} \int dx \left[-y_p \sin(\theta_+ + \zeta) \cos \phi_+ \right. \\ \left. - y_{pn} \cos(\theta_+ + \zeta) \cos \phi_+ \right], \quad (21)$$

$$\begin{pmatrix} y_p(l) \\ y_{pn}(l) \end{pmatrix} = \begin{pmatrix} \cos \zeta & \sin \zeta \\ -\sin \zeta & \cos \zeta \end{pmatrix} \begin{pmatrix} y_{ps}(l) \\ y_{pc}(l) \end{pmatrix}, \quad (22)$$

where $y_p(0) = 4\sqrt{2}\alpha u/v_F$ and $y_{pn}(0) = 0$.

§3. Dimerization vs. CO in the SP state

First, we note the case where the distortion is absent (i.e., $g = 0$ and $x_d \neq 0$). The competition between two kinds of umklapp scattering given by $y_{1/2}$ term and $y_{1/4}$ term is expected with increasing V , since the locking of $\langle \theta_+ \rangle$ of $y_{1/2}$ term and that of $y_{1/4}$ term in eq. (7) becomes different for $V > U/4$. There is a critical value, $V = V_c$, with a fixed U where $y_{1/2}$ becomes relevant (irrelevant) for $V < V_c$ ($V_c < V$) leading to the 1/2-filled state of dimerization (the 1/4-filled state of the CO). The boundary between these two states is shown by the dashed curve in Fig. 1,^{19, 25)} where the dotted curve denotes a boundary for $g = x_d = 0$. It turns out that the region for the CO state is reduced by the dimerization, i.e., x_d due to the competition between $y_{1/4}$ and $y_{1/2}$ terms. The case of $V < V_c$ leads to the Mott-Hubbard state while the case of $V_c < V$ exhibits the CO state. The ground state of the former state is given by $\langle \theta_+ \rangle = \pi/4$ due to the relevant $y_{1/2} (\rightarrow +\infty)$ while that of the latter state is given by $\langle \theta_+ \rangle = \pi/2$ due to the relevant $y_{1/4} (\rightarrow -\infty)$. For both states, the charge excitation is gapfull and the spin excitation is gapless.

Next, we consider the case in the limit of small distortion where the perturbational treatment of the SP state is applicable based on the state with $g = 0$. In this case, the lattice distortion is determined so as to obtain the maximum value of $\sin(\theta_+ + \zeta)$ in eq. (21) since $y_{pn}(0) = 0$. Thus for $V < V_c$ and then $\langle \theta_+ \rangle = \pi/4$, one finds $\zeta = \pi/4$ leading to $2k_F$ BOW and $4k_F$ BOW (the state (a)), while, for $V_c < V$ and then $\langle \theta_+ \rangle = \pi/2$, one finds $\zeta = 0$ lead-

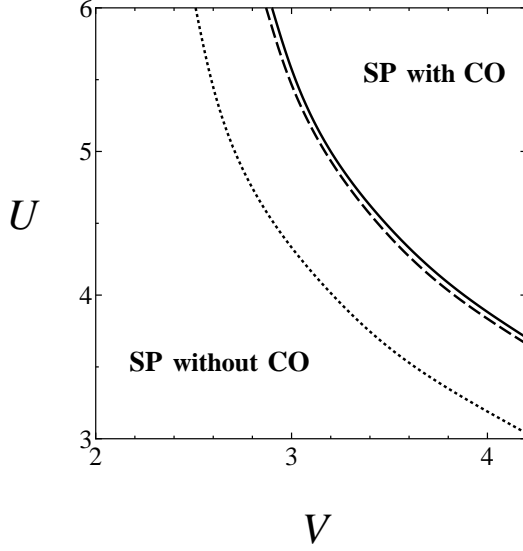


Fig. 1. Phase diagram of an extended Peierls-Hubbard model on the plane of V - U with $x_d = 0.1$ and $g = 0.1$ where the solid curve is a boundary between the spin Peierls (SP) state with CO (charge ordering) and that without CO. A dashed curve (dotted) denotes the boundary for $g \rightarrow 0$ and $x_d = 0.1$ ($g = x_d \rightarrow 0$).

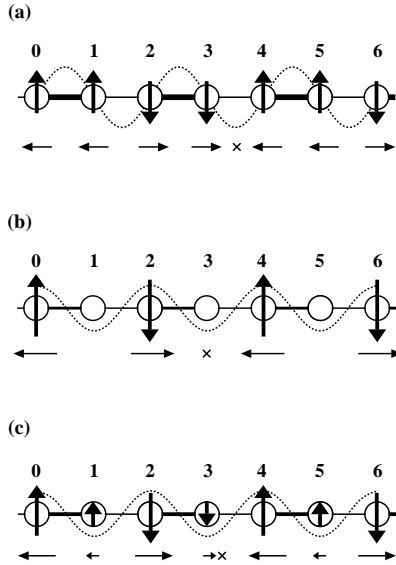


Fig. 2. Spatial variation of the SP state with $\zeta = \pi/4$ for $V < V_c$ (the state (a)), that with $\zeta = 0$ for $V_c \ll V$ (the state (b)) and that with $0 < \zeta < \pi/4$ for $V_c < V$ (the state (c)), respectively. Dotted line denotes the $4k_F$ charge density wave and the vertical arrows (horizontal arrows) denote spin (the lattice displacement). The symbol, \times , is the location for the center of the singlet state.

ing to $2k_F$ CDW and $4k_F$ CDW (the state (b)). These two states are shown in Figs. 2(a) and 2(b), respectively where the arrow denotes a spin and the cross denotes the location for the center of the singlet state. However the presence of the dimerization suggests a possibility of a state given by Fig. 2(c) (the state (c)), i.e., a mixed state with $0 < \zeta < \pi/4$. In this section, we examine not only the states of Figs. 2(a) and 2(b) but also the state of Fig. 2(c) by calculating the optimum ζ , which leads to a

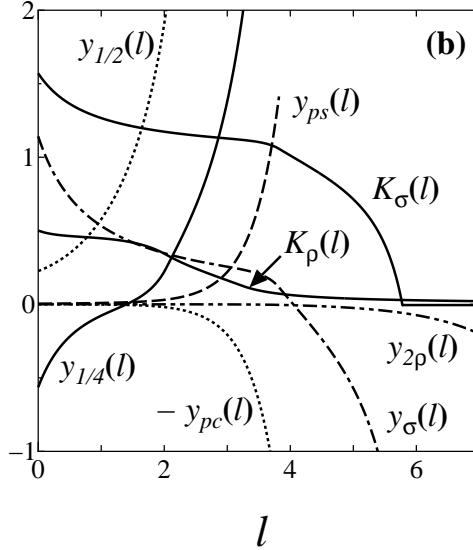
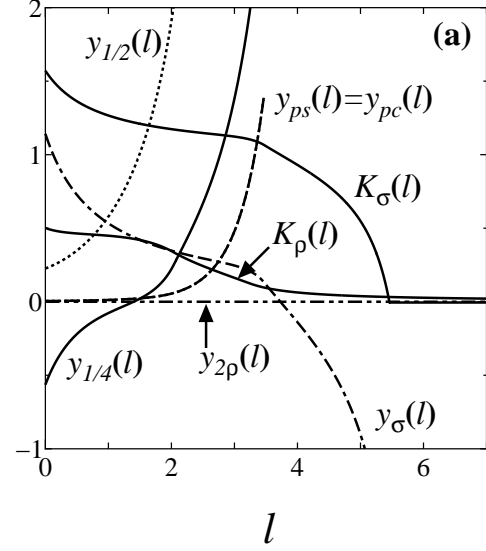


Fig. 3. The l dependence of $K_\rho(l)$, $K_\sigma(l)$, $y_{1/2}(l)$, $y_{1/4}(l)$, $y_{2\rho}(l)$, $y_{2\sigma}(l)$, $y_{ps}(l)$ and $y_{pc}(l)$ for $V = 2$ with $U = 5$, $x_d = 0.1$ and $g = 0.1$ where $\zeta = \pi/4$ ($u = 0.0029$) (a) and $\zeta = 0$ ($u = 0.0018$) (b). Both cases lead to the bond order.

maximum of u and then a minimum of the total energy.

Now we calculate numerically the distortion, u , by taking $t = 1$ and $a = 1$. We choose parameters as $U = 5$, $x_d = 0.1$ and $g = 0.1$ (i.e., $K \simeq 9.05$) and the results for other parameters are discussed later. Figures 3(a) and 3(b), which are obtained from eqs. (16), show the RG flow (i.e., l dependence) for the case of small $V (< V_c)$. The magnitude of u is taken from the solution of eq. (12) where u appears only in the initial value of RG equations. The most relevant quantity is $y_{1/2}$ and then $y_{1/4}(l)$ changes the sign from a negative value to a positive value with increasing l . Figure 3(a) shows $\zeta = \pi/4$ and $\langle \theta_+ \rangle = \pi/4$ due to $y_{ps}(l) = y_{pc}(l)$ while Fig. 3(b) shows $\zeta = 0$ and $\langle \theta_+ \rangle = \pi/4$. Since $\langle \theta_+ \rangle = \pi/4$ regardless the initial condition of ζ , both Figs. 3(a) and 3(b) show $4k_F$ BOW and $2k_F$ BOW. By substituting $y_{ps}(l)$

and $y_{pc}(l)$ of Figs. 3(a) and 3(b) into eq. (22), it turns out that Fig. 3(a) shows the largest $y_p(l)$ indicating the ground state with $\zeta = \pi/4$. The relevant $y_{1/2}$ results in the charge gap determined by the dimerization, which leads to an effectively half-filled band. A spin gap is obtained from the relevant y_σ , which comes from y_{ps} and y_{pc} as seen from eq. (16f). The spin gap is much smaller than the charge gap since $y_{1/2}(l)$ increases rapidly compared with $y_p(l)$.

The RG flows for the case of large $V(> V_c)$ are shown in Figs. 4(a), 4(b) and 4(c) where u is chosen from the solution of eq. (12). In all these figures, $y_{1/2}(l)$ becomes irrelevant due to the relevant $y_{1/4}(l)(< 0)$ indicating $4k_F$ CDW with $\langle\theta_+\rangle = \pi/2$. Figure 4(a) with $\zeta = \pi/4$ shows $y_{ps}(l) = y_{pc}(l)$ which implies $y_p(l) > 0$ and $y_{pn}(l) = 0$. Figure 4(b) with $\zeta = 0$ also shows the relevant y_p and the irrelevant y_{pn} . From the comparison of y_p of Fig. 4(a) and that of Fig. 4(b), it is found that Fig. 4(b) gives the distortion larger than Fig. 4(a). However the larger distortion is expected from the state shown by Fig. 2(c) with $0 < \zeta < \pi/4$, since the dimerization breaks the symmetry around the distortion given by the cross of Fig. 2(b). Actually an example of such a state is shown in Fig. 4(c) where $y_p(l)$ increases rapidly compared with that of Fig. 4(b). For Fig. 4(c), $y_{pn}(l)$ of eq. (22) decreases from zero to a negative value, while $y_{pn}(l) \simeq 0$ for Figs. 3(a) and 4(b). Thus the state for $V > V_c$ is given by Fig. 4(c) with $\zeta > 0$ due to the energy gain from both y_p term and y_{pn} term.

The distortion u is determined by eq. (12), with F estimated from the response function $R(l)$ where eq. (17) is calculated from eqs. (18) and (19). In Fig. 5, the response function $R(l)$ for $\zeta = \pi/4$ is shown for the case of small $V(< V_c)$ (solid curve) and large $V(> V_c)$ (dotted curve), respectively, where $V_c = 3.2$. When the response function enters into the region of forming the charge gap, we stop the RG treatment for the charge fluctuation and take into account only the spin fluctuation by keeping the relevant coupling of eq. (14) as a constant for $l > l_c$. The arrow indicates a location for $l = l_c$ at which the charge fluctuation becomes frozen due to a formation of the charge gap. Finally, we stop calculating the RG equations of eqs. (19) when it takes a minimum at $l = l_m$ (end point) corresponding to the SP state. It is expected that the difference between $R(l_m)$ and the correct value at the long distance is small since the formation of the spin gap occurs at $l \simeq l_m$ due to the SP state. Figure 6 shows u dependence of $F(= R^{1/2}(l_m))$, which is obtained from Fig. 5 with fixed $\zeta = \pi/4$ and some choices of V . The quantity F increases monotonically with increasing u where the power law as a function of u is expected in the presence of the interaction as seen also for the half-filled case.²⁶⁾ It turns out that F takes a maximum as a function of V . Such a maximum originates in a fact that the SP state with $\langle\theta_+\rangle = \pi/4$ is replaced by the CO with $\langle\theta_+\rangle = \pi/2$ in the case of $V > V_c$.

Figure 7 is the main result of the present calculation where the solution u for eq. (12) is obtained from the intersection in Fig. 6. The solid curve corresponds to u for $\zeta = \pi/4$ (Fig. 2(a)) while the dotted curve denotes u for $\zeta = 0$ (Fig. 2(b)). The latter case of $\zeta = 0$ is

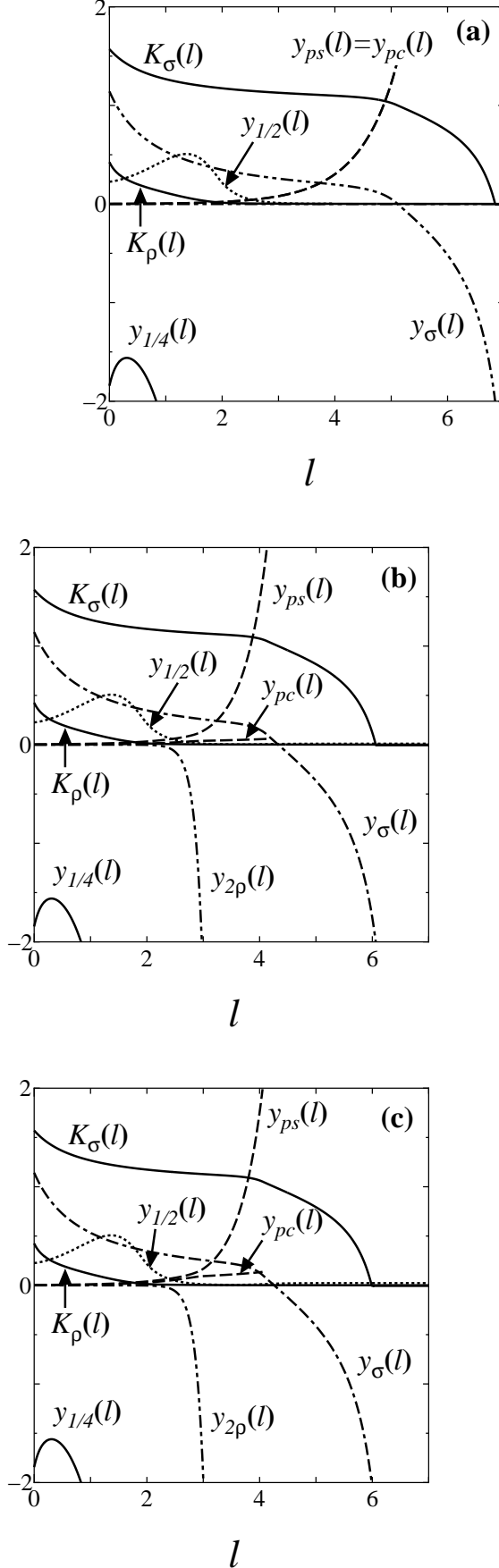


Fig. 4. The l dependence of $K_\rho(l)$, $K_\sigma(l)$, $y_{1/4}(l)$, $y_{1/2}(l)$, $y_{2\rho}(l)$, $y_\sigma(l)$, $y_{ps}(l)$ and $y_{pc}(l)$ for $V = 3.7$ with $U = 5$, $x_d = 0.1$ and $g = 0.1$ where $\zeta = \pi/4$ ($u = 0.0012$) (a), $\zeta = 0$ ($u = 0.0017$) (b) and $\zeta = 0.6 \times \pi/4$ ($u = 0.0020$) (c), respectively. In the first panel (a), $y_{2\rho}(l) = 0$. All these cases lead to the CO due to relevant $y_{1/4}(l) (\rightarrow -\infty)$.

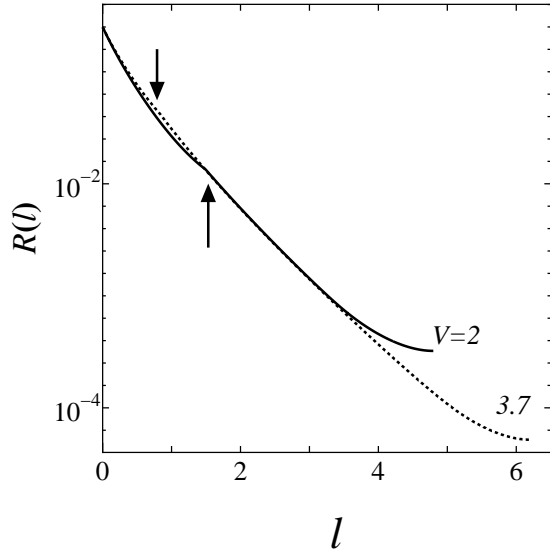


Fig. 5. The l dependence of $R(l)$ for $\zeta = \pi/4$ with $V=2$ (solid curve), 3.7 (dotted curve) where $U = 5, x_d = 0.1$ and $g = 0.1$. The arrow denotes $l(= l_c)$, at which the charge fluctuation is frozen. The end point of $R(l)$ denotes a minimum of $R(l)$ at $l = l_m$.

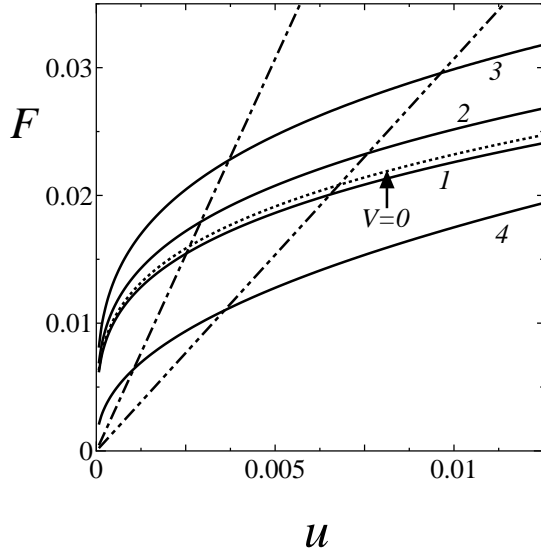


Fig. 6. The quantity F of eq. (12), as the function of u for $\zeta = \pi/4$ with $U = 5, x_d = 0.1$ and $V = 1, 2, 3$ and 4. The dash-dotted (dash-two dotted) line denotes $(\sqrt{2}a/gv_F)u$ of eq. (12) for $g = 0.1$ (0.2), where the solution of eq. (12) is obtained from the intersection.

also calculated in a way similar to Fig. 6. Both curves exhibit a maximum at $V = V_c$ shown by the arrow where the CO state appears for $V > V_c$. The maximum at $V = V_c$ originates in the competition between the dimerization and the CO, which is comprehended as follows. The numerical results together with eqs. (16c) and (16d) show that $y_{1/2}$ becomes irrelevant and $y_{1/4}$ becomes relevant for $V_c < V$. Since the length l for the minimum of $R(l)$ corresponding to u is nearly equal to l with $|y_\sigma(l)| = 2$, the distortion is essentially determined

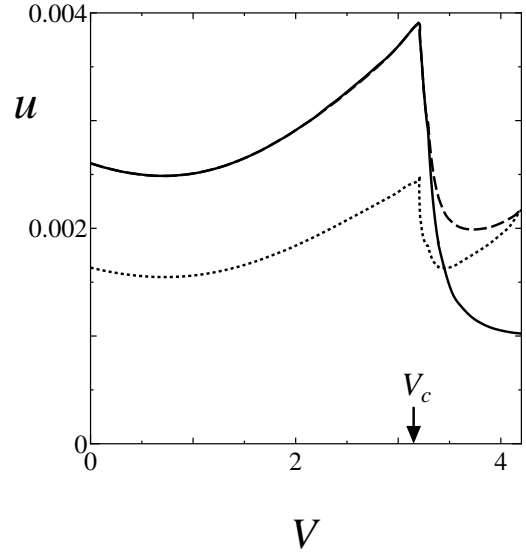


Fig. 7. The V dependence of u for $\zeta = \pi/4$ (solid curve), $\zeta = 0$ (dotted curve) and the optimum value of ζ (dashed curve) where $U = 5, x_d = 0.1$ and $g = 0.1$.

by $[y_{ps}^2(l) + y_{pc}^2(l)]^{1/2}$ in eq. (16f). Equations (16g) and (16h) show that $y_{ps}(l)$ and $y_{pc}(l)$ are determined by the umklapp scatterings, $y_{1/2}(l)$ and $y_{2\rho}(l)$, where $y_{2\rho}$ is induced by $y_{1/4}$ for $V_c < V$ (eq. (16e)). Thus the sudden decrease of u for $V > V_c$ originates in the fact that the increase of $y_{1/2}(l)$ for $V < V_c$ is much larger than that of $y_{2\rho}$ for $V_c < V$, close to $V = V_c$. The increase of u with V just below V_c comes from the decrease of K_ρ , which results in the suppression of the charge fluctuation. From the comparison of the solid curve with the dotted curve, the maximum of u for $V < V_c$ is given by the SP state with $\zeta = \pi/4$ (solid curve) shown in Fig. 2(a),¹³ while u with $\zeta = 0$ (dotted curve) becomes larger than that of the solid curve for large V ($> V_c$). The first order transition might be expected between these two states if the dimerization were absent.¹⁴ However, the mixed state shown in Fig. 2(c) is rather promising for $V > V_c$ since the dimerization does exist even for the SP state with the CO. The dashed curve denotes u of such a mixed state, which is obtained by choosing the optimum ζ leading to the maximum of u . The difference between the dashed curve and the dotted curve becomes small for $V \gtrsim 4$. With increasing V for $V > V_c$, the distortion u increases again since the state of Figs. 4(b) and (c) are compatible with the CO, and K_ρ keeps decreasing with increasing V . The minimum of u for $V < V_c$ comes from the change of the sign of $y_{1/4}(0)$ as the function of V . Thus we obtain the transition from the state of Fig. 2(a) to that of Fig. 2(c) at $V = V_c$.

In Fig. 8, the V dependence of ζ for the mixed state (Fig. 2(c)) is shown where $x_d = 0.1$ (solid curve) and $x_d = 0.2$ (dotted curve). The quantity ζ begins to decrease from $\pi/4$ at a critical value and reduces to zero monotonically. Within the numerical accuracy, the onset of the mixed state is given by $V = V_c$ indicating the second-order transition. With increasing x_d , V_c increases since the SP state with $\zeta = \pi/4$ is enhanced by the dimerization

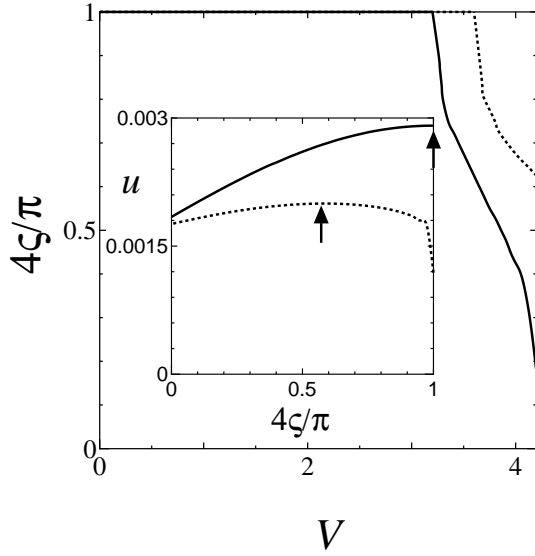


Fig. 8. The V dependence of the optimum ζ for $x_d = 0.1$ (solid curve) and $x_d = 0.2$ (dotted curve) where $U = 5$ and $g = 0.1$. The inset denotes the corresponding ζ dependence of u for $V = 2$ (solid curve) and $V = 3.7$ (dotted curve) for $x_d = 0.1$ where the arrow denotes the location for the optimum ζ .

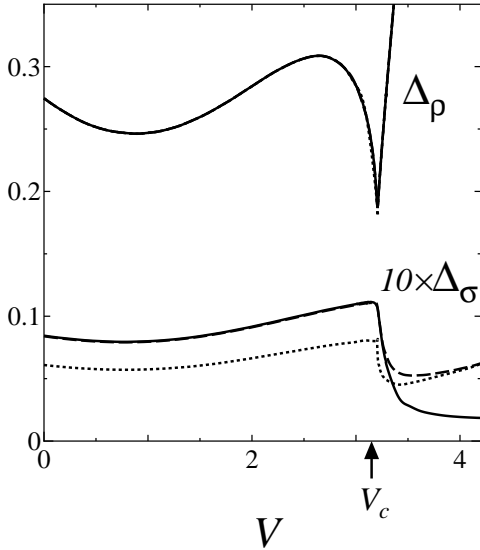


Fig. 9. The V dependence of the charge gap Δ_ρ and the spin gap Δ_σ for $\zeta = \pi/4$ (solid curve), $\zeta = 0$ (dotted curve) and the optimum ζ (dashed curve) where $U = 5$, $x_d = 0.1$ and $g = 0.1$. The difference among three curves of Δ_ρ is invisible. The spin gap, which is multiplied by 10, is similar to u in Fig. 7.

($\propto y_{1/2}$). The inset shows u as a function of ζ where the location of the optimum ζ is shown by the arrow. For $V < V_c$, u as a function of ζ increases monotonically while u for $V_c < V$ takes a maximum in the interval of $0 < \zeta < \pi/4$.

The energy, $v_F \alpha^{-1} \exp(-l_m)$, corresponding to the SP state is nearly equal to that of the freezing of the spin fluctuation while the charge fluctuation is frozen at higher energy as seen from Fig. 5 (the location indicated by the arrow). Figure 9 shows the charge

gap, Δ_ρ , and the spin gap, Δ_σ , which correspond to Fig. 7. These gaps are calculated from $\Delta_\rho = \omega_c \exp[-l_\rho]$ and $\Delta_\sigma = \omega_c \exp[-l_\sigma]$ where $l_\rho = \min(l_{\rho 1}, l_{\rho 2})$ with $y_{1/2}(l_{\rho 1}) = 2$, $|y_{1/4}(l_{\rho 2})| = 3$ and $|y_\sigma(l_\sigma)| = 2$. The cutoff is chosen as $\omega_c = 2.2$, by noting that $\omega_c = 5.3$ for the half-filled case²⁷⁾ and the ratio of the bandwidth of half-filling and that of quarter-filling is 0.41.²⁸⁾ The length l_ρ is essentially the same but is slightly larger than l_c in Fig. 5, which is chosen for the convenience of the numerical calculation of $R(l)$. The charge gap is much larger than the spin gap, which is nearly equal to u . The dip of the charge gap and the cusp of the spin gap, which are found at $V = V_c$, originates in the fact that the fixed point of $y_{1/4}(l)$ changes from $+\infty$ to $-\infty$ at $V = V_c$ (or equivalently from $+\infty$ to 0 for $y_{1/2}(l)$).

Finally, we discuss the relation between the method of obtaining the optimum ζ and that of $\langle \partial H / \partial \zeta \rangle = 0$ shown just above eq. (12). The estimation of the latter one for the state of Fig. 2(c) is very complicated within the present scheme of RG method. However, the condition given by $\langle \partial H / \partial \zeta \rangle = 0$ (i.e., $\langle \cos(\theta_+ + \zeta) \cos \phi_+ \rangle = 0$) seems to be compatible with the former result with $0 < \zeta < \pi/4$ if we note the following property of the quantum fluctuation of θ_+ for $V > V_c$. The fluctuation with low energy (i.e., large l) exists around $\langle \theta_+ \rangle = \pi/2$ due to the fixed point of the CO state while the fluctuation with high energy (i.e., small l) exists around $\langle \theta_+ \rangle = \pi/4$ due to the dimerization as seen from $y_{1/2}(l) \neq 0$ for small l in Fig. 4(c). Further, it should be noted that such a competitor of the dimerization and the CO becomes noticeable for the state with V just above V_c .

§4. Discussion

Using an extended Peierls-Hubbard model where the presence of the dimerization is assumed as a model of organic conductors, we have examined the SP state and obtained the following results. With increasing nearest-neighbor interaction, V , the transition from the SP state of Fig. 2(a) into that of Fig. 2(c) occurs at $V = V_c$ corresponding to the appearance of the CO where the transition is of second-order due to the dimerization. The competition of the dimerization with the CO results in the maximum of u at $V = V_c$ and the rapid decrease of u for V just above V_c .

We have also examined the SP state with other parameters. The calculation of u similar to Fig. 7 for $U = 4, 5$ and 6 shows that u as the function of U decreases monotonically in the region around the maximum (i.e., $V = V_c$) as found for the half-filled case.²⁶⁾ The dimerization x_d increases V_c as seen from Fig. 1 where V_c for $x_d = 0.1$ (solid curve) is much larger than that for $x_d \rightarrow 0$ (dotted curve).^{9, 11)} The SP state without the CO is also enhanced in the presence of g since the SP state of Fig. 2(a) is compatible with the Mott-Hubbard state. The magnitude u of Fig. 7 obtained by $g = 0.1$ is reasonable for the organic conductor in which $t \sim 2000 K$ ¹⁵⁾ and $u(\sim T_{SP}) \sim 10 K$ leading to $u/t \sim 0.005$.¹⁾ The small effect of g on V_c is found from the comparison of the solid curve with the dashed curve in Fig. 1 and from the fact that the enhancement of V_c is about 0.1 even for $g = 0.5$. However, u is strongly enhanced by g . The g

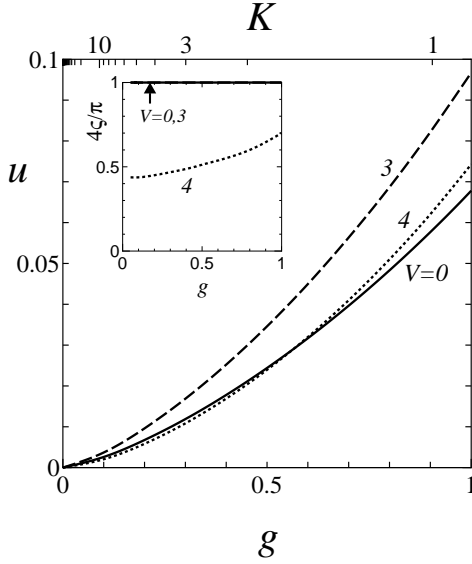


Fig. 10. The g dependence of u for $V = 0, 3$ and 4 with $U = 5$ and $x_d = 0.1$. The inset denotes the optimum ζ corresponding to the main figure.

dependence of u is shown in Fig. 10 with some choices of V . With increasing g , u increases with a power law due to the presence of U while $u \propto \exp(-1/g)$ for the conventional Peierls state (i.e., $U = V = 0$). The V dependence of u is weaker than the g dependence of u . Thus the critical value of V_c in Fig. 7 does not depend much on g indicating also the small effect of g on the boundary in Fig. 1.

We comment on our treatment of the first order RG. We obtained the cusp of u in Fig. 7 and the dip of Δ_ρ in Fig. 9. Such an anomaly originates in the fact that the $y_{1/2}$ term competes with the $y_{1/4}$ term. This competition has a common feature with the Ising transition,^{29,30} which leads to the vanishing of Δ_ρ at $V = V_c$. Thus it is expected that u in Fig. 7 remains finite but the tangent becomes infinity.

Finally, based on the result of Fig. 7 and Fig. 9, we comment on the SP state of organic conductors with the dimerization by noting that $u \propto T_{SP}$, and pressure decreases V/t due to the increase of t . The experiment on $(\text{TMTTF})_2\text{AsF}_6$ ⁵⁾ is interpreted as follows. The SP state under low pressure (< 0.15 GPa), which shows the increase of T_{SP} and the decrease of T_{CO} with increasing pressure, corresponds to the mixed state of Fig. 2(c) obtained for V just above V_c . The SP state under high pressures (> 0.15 GPa) showing the decrease of T_{SP} as the function of pressure, corresponds to the SP state of Fig. 2(a). Further we note the SP state of $(\text{TMTTF})_2\text{X}$ with $\text{X} = \text{PF}_6$ and AsF_6 have $T_{CO} \simeq 62\text{K}$ and 103K and $T_{SP} \simeq 18\text{K}$ and 11K , respectively at ambient pressure.⁵⁾ These two SP states may be described by the mixed state of Fig. 2(c) since V/t of $(\text{TMTTF})_2\text{AsF}_6$ is larger than $(\text{TMTTF})_2\text{PF}_6$ due to the effective pressure.

Acknowledgments

The authors are grateful to M. Ogata and H. Seo for useful comments on the state of Fig. 2(b). They also

thank S. Brasovskii and A. Furusaki for valuable discussions.

Appendix: Renormalization Group Equations

First, we derive the renormalization group (RG) equations for $H^{\text{eff}} = H_0 + H_1^{\text{eff}}$ (eq.(14)), using the response function²¹⁾ given by

$$R(\vec{r}_1 - \vec{r}_2) = \left\langle T_\tau e^{i\theta_+(\vec{r}_1)} e^{-i\theta_+(\vec{r}_2)} \right\rangle_{H^{\text{eff}}} = \frac{1}{\langle S_I \rangle_0} \left\langle T_\tau e^{i\theta_+(\vec{r}_1)} e^{-i\theta_+(\vec{r}_2)} S_I \right\rangle_0. \quad (\text{A.1})$$

T_τ is time ordering operator, $\vec{r} = (x, v_F \tau)$ and $\langle \rangle_0$ denotes the average over H_0 . In the absence of H_1^{eff} , $R(\vec{r}_1 - \vec{r}_2) = \exp\{-K_\rho U(\vec{r}_1 - \vec{r}_2)\}$ with $U(\vec{r}) = \ln(|\vec{r}|/\alpha)$. $S_I = T_\tau \exp[-\int d^2\tilde{r} \tilde{H}_1^{\text{eff}}]$ with $H_1^{\text{eff}} = (v_F/2\pi\alpha^2) \int dx \tilde{H}_1^{\text{eff}}$ and $d^2\tilde{r} = dx v_F d\tau/2\pi\alpha^2$.

We expand the nonlinear terms of H_1^{eff} treating as perturbation and rewrite the response function as $R(\vec{r}_1 - \vec{r}_2) = \exp\{-K_\rho^{\text{eff}} U(\vec{r}_1 - \vec{r}_2)\}$. K_ρ^{eff} is written by $y_{1/4}, y_{1/2}, \dots$. Assuming the scale invariance of response function, one obtain the RG equations.

By expanding \tilde{H}_1^{eff} up to third order, the response function is written as

$$\begin{aligned} R(\vec{r}_1 - \vec{r}_2) = & \exp(-f_\rho(1, 2)) \left[1 + \sum_{\epsilon=\pm} \int d^2\tilde{r}_3 d^2\tilde{r}_4 \right. \\ & \times \left\{ \frac{1}{8} y_{1/4}^2 \exp(-16f_\rho(3, 4)) \{ \exp(4\epsilon[f_\rho(1, 3) \right. \\ & \quad \left. - f_\rho(1, 4) - f_\rho(2, 3) + f_\rho(2, 4)]) - 1 \} \right. \\ & + \frac{1}{8} (y_{1/2}^2 + y_{2\rho}^2) \exp(-4f_\rho(3, 4)) \{ \exp(2\epsilon[f_\rho(1, 3) \\ & \quad \left. - f_\rho(1, 4) - f_\rho(2, 3) + f_\rho(2, 4)]) - 1 \} \\ & + \frac{1}{16} (y_{ps}^2 + y_{pc}^2) \exp\{-f_\rho(3, 4) - f_\sigma(3, 4)\} \\ & \quad \times \{ \exp(\epsilon[f_\rho(1, 3) - f_\rho(1, 4) \\ & \quad \left. - f_\rho(2, 3) + f_\rho(2, 4)]) - 1 \} \} \\ & + \sum_{\epsilon=\pm} \int d^2\tilde{r}_3 d^2\tilde{r}_4 d^2\tilde{r}_5 \left\{ \frac{1}{16} (y_{1/4} y_{1/2}^2 - y_{1/4} y_{2\rho}^2) \right. \\ & \quad \times \exp(-8f_\rho(3, 4) - 8f_\rho(3, 5) + 4f_\rho(4, 5)) \\ & \quad \times \{ \exp(2\epsilon[2f_\rho(1, 3) - f_\rho(1, 4) - f_\rho(1, 5) \\ & \quad \left. - 2f_\rho(2, 3) + f_\rho(2, 4) + f_\rho(2, 5)]) - 1 \} \right. \\ & - \frac{1}{32} (y_{2\rho} y_{ps}^2 - y_{2\rho} y_{pc}^2 - 2y_{1/2} y_{ps} y_{pc}) \\ & \quad \times \exp(-2f_\rho(3, 4) - 2f_\rho(3, 5) + f_\rho(4, 5) - f_\sigma(4, 5)) \\ & \quad \times \{ \exp(\epsilon[2f_\rho(1, 3) - f_\rho(1, 4) - f_\rho(1, 5) \\ & \quad \left. - 2f_\rho(2, 3) + f_\rho(2, 4) + f_\rho(2, 5)]) - 1 \} \\ & - \frac{1}{32} (y_\sigma y_{ps}^2 + y_\sigma y_{pc}^2) \\ & \quad \times \exp(-f_\rho(4, 5) - 2f_\sigma(3, 4) - 2f_\sigma(3, 5) + f_\sigma(4, 5)) \\ & \quad \times \{ \exp(\epsilon[f_\rho(1, 4) - f_\rho(1, 5) \end{aligned}$$

$$\left. -f_\rho(2, 4) - f_\rho(2, 5)] - 1 \} \right\} \Bigg] , \quad (\text{A.2})$$

where $f_{\rho(\sigma)}(i, j) = K_{\rho(\sigma)} U(\vec{r}_i - \vec{r}_j)$. Noting the renormalization form, one obtain

$$\begin{aligned} y_{1/4}^{\text{eff}} &= y_{1/4} + \frac{1}{4} (y_{1/2}^2 - y_{2\rho}^2) \int_\alpha^\infty \frac{dr}{\alpha} \left(\frac{r}{\alpha} \right)^{1+4K_\rho} , \\ y_{1/2}^{\text{eff}} &= y_{1/2} + \frac{1}{2} y_{1/4} y_{1/2} \int_\alpha^\infty \frac{dr}{\alpha} \left(\frac{r}{\alpha} \right)^{1-8K_\rho} \\ &\quad + \frac{1}{4} y_{ps} y_{pc} \int_\alpha^\infty \frac{dr}{\alpha} \left(\frac{r}{\alpha} \right)^{1+K_\rho-K_\sigma} , \\ y_{2\rho}^{\text{eff}} &= y_{2\rho} - \frac{1}{2} y_{1/4} y_{2\rho} \int_\alpha^\infty \frac{dr}{\alpha} \left(\frac{r}{\alpha} \right)^{1-8K_\rho} \\ &\quad - \frac{1}{8} (y_{ps}^2 - y_{pc}^2) \int_\alpha^\infty \frac{dr}{\alpha} \left(\frac{r}{\alpha} \right)^{1+K_\rho-K_\sigma} , \\ y_{ps}^{\text{eff}} &= y_{ps} + \frac{1}{2} (y_{1/2} y_{pc} - y_{2\rho} y_{ps}) \int_\alpha^\infty \frac{dr}{\alpha} \left(\frac{r}{\alpha} \right)^{1-2K_\rho} \\ &\quad - \frac{1}{2} y_\sigma y_{ps} \int_\alpha^\infty \frac{dr}{\alpha} \left(\frac{r}{\alpha} \right)^{1-2K_\sigma} , \\ y_{pc}^{\text{eff}} &= y_{pc} + \frac{1}{2} (y_{1/2} y_{ps} + y_{2\rho} y_{pc}) \int_\alpha^\infty \frac{dr}{\alpha} \left(\frac{r}{\alpha} \right)^{1-2K_\rho} \\ &\quad - \frac{1}{2} y_\sigma y_{pc} \int_\alpha^\infty \frac{dr}{\alpha} \left(\frac{r}{\alpha} \right)^{1-2K_\sigma} . \end{aligned} \quad (\text{A.3})$$

By reexponentiating the renormalized form of eq. (A.2), one obtain

$$R(\vec{r}_1 - \vec{r}_2) = \exp \left(-K_\rho^{\text{eff}} U(\vec{r}_1 - \vec{r}_2) \right) , \quad (\text{A.4})$$

where

$$\begin{aligned} K_\rho^{\text{eff}} &= K_\rho - \left[2 y_{1/4}^2 \int_\alpha^\infty \frac{dr}{\alpha} \left(\frac{r}{\alpha} \right)^{3-16K_\rho} \right. \\ &\quad - \frac{1}{2} (y_{1/2}^2 + y_{2\rho}^2) \int_\alpha^\infty \frac{dr}{\alpha} \left(\frac{r}{\alpha} \right)^{3-4K_\rho} \\ &\quad \left. - \frac{1}{16} (y_{ps}^2 + y_{pc}^2) \int_\alpha^\infty \frac{dr}{\alpha} \left(\frac{r}{\alpha} \right)^{3-K_\rho-K_\sigma} \right] K_\rho^2 . \end{aligned} \quad (\text{A.5})$$

From the condition of scale invariance for $\alpha \rightarrow \alpha(1+dl)$, we obtain the RG equations of $K_\rho, K_\sigma, y_{1/4}, y_{1/2}, y_{2\rho}, y_{ps}$ and y_{pc} in eqs. (16). RG equations for K_σ and y_σ are obtained in a similar way from the response function, $R(\vec{r}_1 - \vec{r}_2) = \langle T_\tau e^{i\phi_+(\vec{r}_1)} e^{-i\phi_+(\vec{r}_2)} \rangle_{H^{\text{eff}}}$.

Next, we derive the RG equation of response function²³⁾ R_s written as

$$\begin{aligned} R_s(\vec{r}_1 - \vec{r}_2) &= \langle T_\tau \sin \theta_+(\vec{r}_1) \cos \phi_+(\vec{r}_1) \sin \theta_+(\vec{r}_2) \cos \phi_+(\vec{r}_2) \rangle_{H^{\text{eff}}} . \end{aligned} \quad (\text{A.6})$$

We calculate R_s up to the second order in H_1^{eff} . In a way similar to RG equations, one obtain

$$R_s(\vec{r}_1 - \vec{r}_2) = \frac{1}{4} \exp(-f_\rho(1, 2) - f_\sigma(1, 2)) \times \tilde{R}_s(\vec{r}_1 - \vec{r}_2) ,$$

where

$$\begin{aligned} \tilde{R}_s(\vec{r}_1 - \vec{r}_2) &= 1 - \frac{1}{2} \int_\alpha^\infty d^2 \tilde{r}_3 \\ &\times \left\{ y_{2\rho} \exp(2[f_\rho(1, 2) - f_\rho(1, 3) - f_\rho(2, 3)]) \right. \\ &\quad + y_\sigma \exp(2[f_\sigma(1, 2) - f_\sigma(1, 3) - f_\sigma(2, 3)]) \Big\} \\ &\quad + \left[\left\{ 2 y_{1/4}^2 \int_\alpha^\infty \frac{dr}{\alpha} \left(\frac{r}{\alpha} \right)^{3-16K_\rho} \right. \right. \\ &\quad + \frac{1}{2} (y_{1/2}^2 + y_{2\rho}^2) \int_\alpha^\infty \frac{dr}{\alpha} \left(\frac{r}{\alpha} \right)^{3-4K_\rho} \\ &\quad + \frac{1}{16} (y_{ps}^2 + y_{pc}^2) \int_\alpha^\infty \frac{dr}{\alpha} \left(\frac{r}{\alpha} \right)^{3-K_\rho-K_\sigma} \Big\} K_\rho^2 \\ &\quad + \left\{ \frac{1}{2} y_\sigma^2 \int_\alpha^\infty \frac{dr}{\alpha} \left(\frac{r}{\alpha} \right)^{3-4K_\sigma} \right. \\ &\quad \left. \left. + \frac{1}{16} (y_{ps}^2 + y_{pc}^2) \int_\alpha^\infty \frac{dr}{\alpha} \left(\frac{r}{\alpha} \right)^{3-K_\rho-K_\sigma} \right\} K_\sigma^2 \right] \\ &\times U(\vec{r}_1 - \vec{r}_2) . \end{aligned} \quad (\text{A.8})$$

The scale transformation, $\alpha \rightarrow \alpha' = \alpha(1+dl)$, leads to ($r = |\vec{r}_1 - \vec{r}_2| = \alpha e^l$)

$$\tilde{R}_s(r, \alpha) = I(dl) \tilde{R}_s(r, \alpha') , \quad (\text{A.9})$$

where

$$\begin{aligned} I(dl) &= \exp \left[-y_{2\rho} dl - y_\sigma dl \right. \\ &\quad + \left\{ \left(2y_{1/4}^2 + \frac{1}{2} (y_{1/2}^2 + y_{2\rho}^2) + \frac{1}{16} (y_{ps}^2 + y_{pc}^2) \right) K_\rho^2 \right. \\ &\quad \left. \left. + \left(\frac{1}{2} y_\sigma^2 + \frac{1}{16} (y_{ps}^2 + y_{pc}^2) \right) K_\sigma^2 \right\} U(\vec{r}_1 - \vec{r}_2) dl \right] . \end{aligned} \quad (\text{A.10})$$

From eqs. (A.7), (A.9) and (16), we obtain

$$\begin{aligned} R_s(r) &= \frac{1}{4} \exp \left[- \int_0^{\ln(r/\alpha)} dl \{ K_\rho(l) + K_\sigma(l) + y_{2\rho}(l) + y_\sigma(l) \} \right] , \end{aligned} \quad (\text{A.11})$$

which leads to

$$\frac{d}{dl} R_s(l) = - [K_\rho(l) + K_\sigma(l) + y_{2\rho}(l) + y_\sigma(l)] R_s(l) . \quad (\text{A.12})$$

We note that the additional term coupled to R_{sc} can be calculated in terms of the operator product expansion.²⁴⁾

- 1) K. Bechgaard and D. Jerome: *Physica Scripta* **39** (1991) 37.
- 2) D.S. Chow, F. Zamborszky, B. Alavi, D.J. Tantillo, A. Baur, C.A. Merlic and S.E. Brown: *Phys. Rev. Lett* **85** (2000) 1698.
- 3) F. Nad, P. Monceau, C. Carcel and J.M. Fabre: *Phys. Rev. B* **62** (2000) 1753.
- 4) P. Monceau, F.Ya. Nad and S. Brazovskii: *Phys. Rev. Lett* **86** (2001) 4080.
- 5) F. Zamborszky, W. Yu, W. Raas, S.E. Brown, B. Alavi, C.A. Merlic and A. Baur: *Phys. Rev. B* **66** (2002) 081103.
- 6) K.C. Ung, S. Mazumdar and D. Toussaint: *Phys. Rev. Lett* **73** (1994) 2603.
- 7) J. Riela and D. Poilblanc: *Phys. Rev. B* **62** (2000) 0112278.
- 8) R.T. Clay, S. Mazumdar and D.K. Campbell: *cond-mat/0112278*.
- 9) F. Mila and X. Zotos: *Europhys. Lett.* **24** (1993) 133.
- 10) H. Seo and H. Fukuyama: *J. Phys. Soc. Jpn.* **66** (1997) 1249.
- 11) H. Yoshioka, M. Tsuchiizu and Y. Suzumura: *J. Phys. Soc. Jpn.* **69** (2000) 651.
- 12) Y. Suzumura: *J. Phys. Soc. Jpn.* **66** (1997) 3244.
- 13) M. Sugiura and Y. Suzumura: *Proc. 23rd Int. Conf. Low Temp. Phys., Hiroshima, 2002*.
- 14) H. Seo, M. Kuwabara and M. Ogata: *Read at the Meetings of the Physical Society of Japan at Kasugai on September 6-9, 2002* ; M. Kuwabara, H. Seo and M. Ogata: *J. Phys. Soc. Jpn.* **72** (2003) 225.
- 15) L. Ducasse, M. Abderrabba, J. Hoarau, M. Pesquer, B. Gallois and J. Gaultier: *J. Phys. C* **19** (1986) 3805.
- 16) Y. Suzumura: *Prog. Theor. Phys.* **61** (1979) 1.
- 17) A. Luther and I. Peschel: *Phys. Rev. B* **9** (1974) 2911.
- 18) D.C. Mattis and E.H. Lieb: *J. Math. Phys.* **6** (1965) 304.
- 19) M. Tsuchiizu, H. Yoshioka and Y. Suzumura: *J. Phys. Soc. Jpn.* **70** (2001) 1460.
- 20) J. Sólyom: *Adv. Phys.* **28** (1979) 201.
- 21) T. Giamarchi and H.J. Schulz: *J. Phys. France* **49** (1988) 819.
- 22) K. Yonemitsu : *Phys. Rev B* **56** (1997) 7262.
- 23) T. Giamarchi and H.J. Schulz: *Phys. Rev. B* **39** (1989) 4620.
- 24) J. L. Cardy, *Scaling and Renormalization in Statistical Physics, Cambridge Lecture Notes in Physics* (Cambridge University Press, Cambridge, UK, 1996).
- 25) Y. Shibata, S. Nishimoto and Y. Ohta: *Phys. Rev. B* **64** (2001) 235107.
- 26) M. Sugiura and Y. Suzumura: *J. Phys. Soc. Jpn.* **71** (2002) 697.
- 27) E.H. Lieb and F.Y. Wu: *Phys. Rev. Lett* **20** (1968) 1445.
- 28) M. Tsuchiizu and Y. Suzumura: *J. Phys. Soc. Jpn.* **68** (1999) 3966.
- 29) M. Fabrizio, A.O. Gogolin, A.A. Nersesyan : *Nucl. Phys. B* **580** (2000) 647.
- 30) M. Tsuchiizu and E. Orignac : *J. Phys. Chem . Solids.* **63** (2002) 1459.